Taylor & Francis
Taylor & Francis Group

RESEARCH ARTICLE

☐ OPEN ACCESS Check for updates

Bioactive constituents of *Salvia przewalskii* and the molecular mechanism of its antihypoxia effects determined using quantitative proteomics

Yafeng Wang[a], Delong Duo[a], Yingjun Yan[a], Rongyue He[a], Shengbiao Wang[a], Aixia Wang[a] and Xinan Wu[b]

[a]People's Hospital of Qinghai Province, Xining, China; [b]Department of Pharmacy, The First Hospital of Lanzhou University, Lanzhou, China

ABSTRACT

Context: Environmental hypobaric hypoxia induces several physiological or pathological responses in individuals in high-altitude regions. *Salvia przewalskii* Maxim (Labiatae) (SPM) is a traditional Chinese herbal medicine and has known antibacterial, antiviral, antioxidant, anti-thrombotic, and anti-depressant activities.

Objective: This study examined the antihypoxia effects of SPM *in vivo*.

Materials and methods: The dried and pulverised of SPM was extracted from root crude drug with 70% ethanol with ultrasound. Male Sprague-Dawley rats were divided into three groups ($n = 10$): normal group, hypoxia group (altitude of 4260 m), and hypoxia + SPM group (altitude of 4260 m, SPM of 1.0 g/kg/day). The experiment persisted for 4 weeks. The mean pulmonary arterial pressure (mPAP), hypoxia-inducible factor-1α (HIF-1α) mRNA, and lung pathology were analysed using pulmonary artery pressure recorder, quantitative polymerase chain reaction, and histopathological analysis. Moreover, the effects of SPM on lung proteomes during hypoxia were observed by a TMT-based proteomic approach.

Results: Pre-treatment with SPM decreased mPAP (24.86%) and HIF-1α (31.24%), and attenuated the pathological changes in lung tissues. In addition, a total of 28 proteins were differentially expressed in lung of hypoxia + SPM group (fold change $> \pm 1.2$ and $p < 0.05$). The differentially altered proteins were primarily associated with antioxidative stress, as evidenced by the downregulated expression of Adh7, Cyp2d1, Plod2, Selenow, ND3, and Fabp1, and fructose metabolism, as evidenced by the downregulated expression of Khk and Aldob.

Discussion and conclusions: These results suggested that SPM is a promising drug for antihypoxia. The mechanism of action might be related to increasing antioxidant capacity and inhibiting fructose metabolism.

Introduction

Approximately 140 million people live in plateau areas at high altitudes (>2500 m) (Pratali et al. 2010). The Qinghai-Tibetan Plateau, known as the 'Roof of the World', is the largest and highest plateau in the world, with an average altitude of >4000 m above sea level (Yang et al. 2018). Currently, more than ten million people ordinarily reside at Qinghai-Tibetan Plateau. In addition, increasing numbers of people who live in low altitude areas migrate to the plateau for travel or work. Acute exposure to high altitude may cause acute mountain sickness [dizziness, nausea, palpitation, shortness of breath, high-altitude pulmonary edoema, high-altitude cerebral edoema and high-altitude pulmonary hypertension (HAPH)] (Barry and Pollard 2003; Beall et al. 2010). HAPH is a severe health consequence of chronic exposure to hypobaric hypoxia, with a frequent occurrence of 15% in high-altitude regions (Leon-Velarde et al. 2005). HAPH is characterised by increased pulmonary vascular resistance, pulmonary vasoconstriction and vascular remodelling of pulmonary arterioles (Beall et al. 2010), and HAPH is the leading cause of death from altitude sickness (Hackett and

Roach 2001). Currently, there are no efficacious therapeutic treatments for HAPH. Therefore, it is important and necessary to develop novel medicines to improve treatments for HAPH-associated sicknesses.

Salvia przewalskii Maxim (Labiatae) (SPM) is mainly produced in the western regions of China (Gansu, Qinghai, and Tibet). The main pharmacological activities of SPM are similar to those of *Salvia miltiorrhiza* Bunge, which is a well-known traditional Chinese medicine with pharmacological functions that can be used to treat angina pectoris, stroke, atherosclerosis, myocardial infarction, liver fibrosis and hepatitis in clinical practice (Fei et al. 2017; Yu et al. 2018). Dripping pills of *S. miltiorrhiza* were approved for phase III clinical trials by the Food and Drug Administration (FDA) (Hao et al. 2015; Jia et al. 2018), while SPM has not been included in the 'Chinese Pharmacopoeia'. The pharmacological activity of SPM is not completely clear and urgently needs to be detected.

Here, we report the antihypoxia activity and mechanism of SPM. Proteins are key to the biological function. Proteomics has been increasingly widely used in traditional medicine research (Olson et al. 2010; Ribon et al. 2016). The combination of

---

proteomics and bioinformatics analysis provides a new way to gain insight into the targets, mechanisms and effective components of natural herbs. This research aimed to study changes in specific protein expression levels or protein species in the lungs of high-altitude rats and SPM-treated hypoxia rats in response to high-altitude hypobaric hypoxia by using tandem mass tag (TMT)-based quantitative proteomics analysis. We hope to find potential target proteins to better understand SPM's antihypoxia mechanism.

Materials and methods

Preparation of SPM suspension

SPM roots were collected from Minhe (Qinghai Province, China), in October 2018, and identified by DD (one of the authors). The voucher specimen (20181011) was deposited in People's Hospital of Qinghai Province. The SPM was cleaned, dried, pulverised, and extracted with 70% ethanol with ultrasound (power, 180 W; frequency, 40 kHz) for 50 min. The extract solution was centrifuged, dried and ground to obtain the extract powder. The desired concentration of SPM suspension was prepared by dissolving the extract powder with deionised water.

Detection of the major active components of SPM by HPLC

The SPM extract powder was dissolved with 500 μL of 80% methanol and then filtered through a 0.22 μm nylon mesh into sample vials. The test sample and mixed standard sample analyses were performed with an Agilent 1290 Infinity LC system coupled to an ultraviolet-visible (UV-vis) detector (Agilent, USA). Chromatographic separation of test samples and mixed standard samples was performed on a SunFire C-18 threaded column (4.6 × 250 mm, 5.0 μm, Waters, USA) maintained at 26 °C. The mobile phase consisted of solvent A (0.1% formic acid in acetonitrile, v/v) and B (0.1% formic acid in water, v/v). The post time was set to 3 min for equilibration. The SPM detection method was further validated by inspecting the linear range, precision, repeatability, and recovery rate according to FDA guidance for the validation of bioanalytical methods.

Animal experiments

Thirty male SPF-grade Sprague-Dawley (SD) rats (7 weeks old, weighing 160–180 g) were purchased from the Experimental Animal Centre of Xi'an Jiaotong University (license key: SCXK (Shaanxi) 2017-003). All rats were housed in facilities with a controlled relative humidity (45–65%), temperature (22 ± 2 °C) and a 12 h light/dark cycle. Feed and drinking water were supplied to the rats *ad libitum*. All rats were randomly assigned to three groups ($n = 10$): (I) normal group (the rats were raised in Xining; altitude, approximately 2260 m); (II) hypoxia group (the rats were raised in Maduo; altitude, approximately 4260 m); (III) hypoxia + SPM groups (the rats were administered a dose of SPM (1.0 g/kg body weight every day) by gavage and raised in Maduo; altitude, approximately 4260 m). The experiment persisted for 4 weeks.

At the end of the experiments, all animals were anaesthetised with phenobarbital (intraperitoneal injection, 30 mg/kg), and the mean pulmonary arterial pressure (mPAP) was detected by a pulmonary artery pressure recorder. All animals were sacrificed under anaesthesia, and the lungs were immediately carefully isolated. Some tissues were fixed with 10% formalin, dehydrated with gradient alcohol, embedded in paraffin, sliced with a microtome and stained with haematoxylin and eosin (H&E) for pathological observations by light microscopy. Some lung tissues were frozen in liquid nitrogen and then transferred and stored at −80 °C until analysis. Some lung tissues were homogenised with a tissue homogeniser at 4 °C, and then the homogenate was centrifuged at 10,000 rpm for 10 min at 4 °C. The supernatant was transferred to a new tube and stored at −80 °C until analysis. The concentrations of malondialdehyde (MDA) and superoxide dismutase (SOD) were detected using commercial kits according to the manufacturer's protocols (the two kits were purchased from Nanjing Jiancheng Bioengineering Institute, Nanjing, China).

Protein extraction

Six samples of lung tissues from the hypoxia + SPM and hypoxia groups were processed individually, and each group had three rats. Each lung tissue was treated with SDT (4% SDS, 100 mM Tris-HCl, pH 7.6) and transferred to a Lysing Matrix A tube, and an MP homogeniser was used to crush the sample (24 × 2, 6.0 M/S, 60 s, twice). After ultrasound, the samples were incubated in a boiling water bath for 10 min. Then, the samples were centrifuged at 14,000 g for 15 min. Finally, the supernatant was collected and filtered using a 0.22 μm centrifuge tube filter. The protein concentration was quantified by a BCA kit (Beyotime, Shanghai, China) (Zhu et al. 2014). The samples were packed and stored at −20 °C.

SDS-PAGE

A 6X loading buffer solution (Beyotime, Shanghai, China) was added to each protein sample (50 μg), and the samples were processed in a boiling water bath for 5 min. Then, the samples were loaded onto 12% SDS-PAGE and subjected to electrophoresis at 250 V for 40 min. The gels were stained with a solution containing Coomassie brilliant blue.

FASP enzymolysis

For digestion, 5 mM dithiothreitol (DTT, 43819-5 G, Sigma) was added to the protein solution (200 μg), and the mixture was incubated for 5 min in boiling water. The samples were then naturally cooled to room temperature. Next, 200 μL of UA buffer (8 M urea, 150 mM Tris-HCl, pH 8.5) was used to remove the DTT and detergent components by ultrafiltration (30 kD), followed by centrifugation at 12,500 g for 25 min (repeated this step twice). Subsequently, 100 μL of iodoacetamide (IAA) buffer was added to the concentrate, followed by centrifugation at 12,500 g for 25 min. Then, 100 μL of UA buffer was added to the resulting concentrate, the sample was centrifuged at 12,500 g for 15 min, and this step was repeated two additional times. Afterwards, 100 μL of 0.1 M triethylammonium bicarbonate (TEAB, SE252676/90114, Thermo) was added, followed by centrifugation at 12,500 g for 15 min, and this step was repeated two times. Finally, the protein suspensions were digested for 16–18 h at 37 °C with 40 μL of trypsin buffer (4 μg trypsin in 40 μL of 0.1 M TEAB). Finally, the sample was centrifuged at 12,500 g for 15 min, and the filtrate was collected (Wiśniewski et al. 2009; Wang et al. 2017).

Table 1. Target gene information and primers for real-time PCR.

Target gene	Primer sequence (5′→3′)		Amplicon size (bp)
	F	R	
HIF-1α	CCAGATTCAAGATCAGCCAGCA	GCTGTCCACATCAAAGCAGTACTCA	162
Mmp8	CCACTTACCAAGCAATCAG	GAGTTAGCAAGAAATCACC	179
Fabp1	TTCTCCGGCAAGTACCAAG	TCTCCAGTTCGCACTCCTC	211
Bmi1	TTAGTTCCAGGGCTTTTCA	ACCTCCTCCTTTGGCTTCT	224
Aldob	TTGCCAATGGGAAGGGTAT	GAGCGTCTCATGGAAAAGG	182
Adh7	TATCACCCdTGAAATCCCG	TaCCACTCGCTGcTAATGC	122
Khk	GATTTATTAACCGACATCTG	CTCGATCTACCTTGACATC	230
Gapdh	TTCAACGGCACAGTCAAGG	CTCAGCACCAGCATCACC	114

TMT labelling, HPLC fractionation and LC − MS/MS

After trypsin digestion, 100 μg of peptide was taken from each sample and labelled according to TMT (Tandem Mass Tag) 6 plex Isobaric Mass Tag Labelling kit protocol (Thermo Fisher Scientific, Torrance, CA, USA). The samples were labelled as follows: A1:126, A2:127, A3:128, B1:129, B2:130, and B3:131. The labelled samples were subsequently fractionated by high pH reverse-phase high-performance liquid chromatography (Agilent 1260 infinity II HPLC). The samples were added to a C18-reversed phase column (Thermo Fisher Scientific) in buffer A (10 mM $HCOONH_4$, 5% ACN, pH 10.0) and then separated with buffer B (10 mM $HCOONH_4$, 85% ACN, pH 10.0). The peptides were separated using a flow rate of 300 nL/min. The chromatographic column was balanced with buffer A, the sample was loaded using an automatic sampler, and the flow rate was 1 mL/min. The gradient profile was 0–7% B from 0 min to 65 min, 7–40% B from 65 min to 70 min and 10–100% B from 70 min to 85 min. The fractions were combined and then vacuum-dried. The dried samples were subsequently reconstituted and evaluated by LC-MS/MS (Thermo Fisher Scientific), and the detailed procedures of the LC-MS/MS methodology were performed as previously described (Wang et al. 2017; 2019). An MS^1 survey scan of 350–1800 m/z at a resolution of 70,000 was collected with an AGC target of 3.0×106 and maximum injection time of 50 millisecond (ms). Following fragmentation, the MS^2 precursor population was selected using the SPS waveform (10 notches) and then fragmented by HCD (2 m/z isolation window, maximum injection time of 45 ms, resolution of 35,000, microscans of 1, normalised collision energy of 30 eV).

MS/MS data analysis and bioinformatics analysis

The raw MS/MS data were input into the Mascot 2.6 and Proteome Discoverer 2.1 databases with a false discovery rate (FDR) < 0.01 at the protein and peptide levels. The search parameters included 6 plex TMT, allowing 2 missing cleavages by cleavage enzyme trypsin, fixed modification (carbamidomethyl) and variable modification (oxidation, protein N-term acetylation). The mass error was set to 10 ppm in the first search, and the fragment ions of mass tolerance were set to 0.05 Da. All identified proteins had ≥2 peptides with ≥1 unique peptide, and only the proteins at $p < 0.05$ were considered to be accurately quantified. For the comparison between the hypoxia + SPM and hypoxia groups, a protein with a fold change of $> \pm 1.2$ and a p-value of <0.05 was regarded as a differentially expressed protein. The Blast2GO database provided Gene Ontology (GO) annotation data. The Kyoto Encyclopaedia of Genes and Genomes (KEGG) database was used to perform pathway enrichment analysis. Protein-protein interaction (PPI) networks were identified and visualised with the IntAct (http://www.ebi.ac.uk/ intact/main.xhtml) database and Cytoscape software (version 3.2.1), respectively.

RNA extraction and real-time quantitative PCR

The total mRNA was isolated from the lung using the Trizol reagent (TaKaRa, Dalian, China) following the manufacturer's protocol. Complementary DNA synthesis was performed using a HiScript 1st Strand cDNA Synthesis Kit (TaKaRa, Dalian, China). Real-time quantitative PCR (RT-qPCR) was used to detect hypoxia-inducible factor-1α (HIF-1α) with the ABI-7900HT system (Applied Biosystems) ($n = 10$). The Mmp8, Fabp1, Bmi1, Aldob, Adh7 and Khk genes were also evaluated by RT-qPCR to validate the proteomics results ($n = 6$). The relative expression of genes was calculated using the $2^{-\triangle\triangle Ct}$ method. The details of the primers used are listed in Table 1.

Statistical analysis

Statistical analysis was performed using GraphPad Prism 5.0 software (GraphPad, CA, USA). The comparison of means of three groups was carried out using one-way analysis of variance (ANOVA), and differences between two groups were determined by unpaired two-tailed Student's t-test. For volcano plot, histogram and clustering analysis, the proteomics data were log transformed and normalised when appropriate. For enrichment analysis, Fisher's exact test was applied. p-Values less than 0.05 were considered statistically significant (*p-value <0.05; **p-value <0.01; and ***p-value <0.001; ns: not significant, p-value >0.05).

Results

The major components of SPM and its significant antihypoxia effects

HPLC analysis showed that the major components and contents of SPM extract were rosmarinic acid (4.334%) and salvianolic acid B (2.526%) (Figure 1(A,B)). The hypoxia experiments were performed at an altitude of 4260 m. The hypoxia rats showed poor diet, polypnea and less active, but the hypoxia + SPM rats reversed the hypoxia phenotype. And the results showed that mPAP was significantly increased in the hypoxia groups compared with the control group ($p < 0.001$) (Figure 1(C)). The number of alveoli and the alveolar space were reduced, the structure was disordered, red blood cells leaked, the alveolar septum was thickened, the capillary was seriously congested and the wall of the tubes was thickened in the lung in the hypoxia groups (Figure 1(D)). HIF-1α activation is well known to be induced by hypoxia, and HIF-1α is a marker of hypoxia (Soeda et al. 2009). In our study, the level of HIF-1α mRNA was significantly
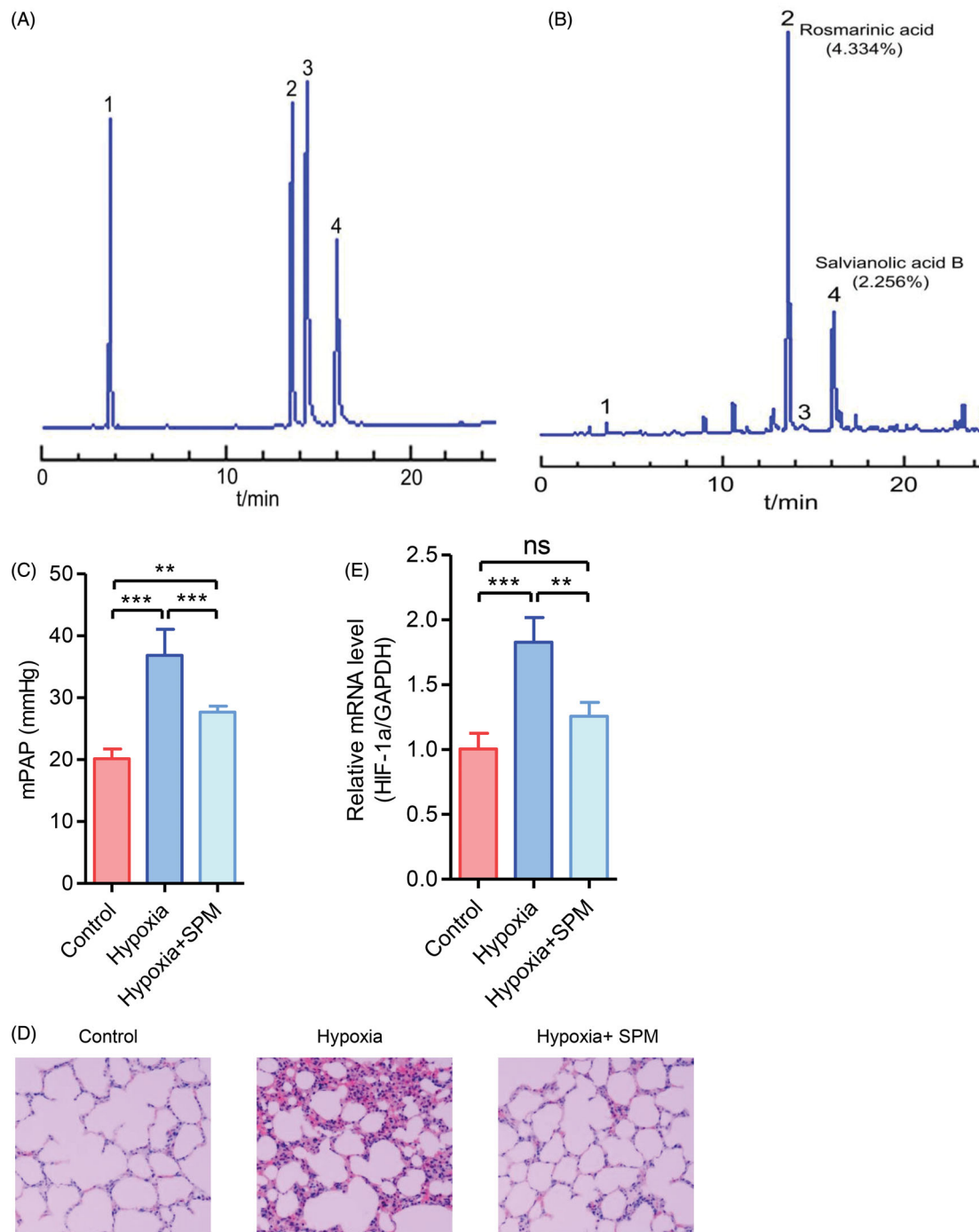
Figure 1. SPM showed significant antihypoxia effects. (A) HPLC chromatogram of mixed standard solutions. (B) HPLC chromatogram of SPM extract. (C) Oral administration of SPM for 4 weeks significantly decreased the levels of mPAP compared with Hypoxia groups ($n = 10$). (D) H&E staining of lung in different groups (×200) ($n = 10$). (E) The effects of SPM on HIF-1α mRNA expressions in lung by RT-qPCR ($n = 10$). ***$p < .001$, **$p < .01$, ns: not significant, $p > .05$.

increased in the rats in the hypoxia group compared with those in the control groups ($p < 0.001$) as detected by RT-qPCR (Figure 1(E)). All of these results indicated that feeding rats for 4 weeks at an altitude of 4260 m led to HAPH pathology and lesions. However, as indicated in Figure 1(C–E), compared with hypoxia, SPM markedly decreased mPAP and HIF-1α ($p < 0.001$ or .01); these results were further confirmed by pathology examination. As shown in Figure 1(D), the lung pathology in the hypoxia + SPM group was clearly improved and showed basically normal organisational form and structure. These results indicated that SPM has clear antihypoxia effects.

Data analysis and protein identification

To investigate the antihypoxia mechanisms of SPM, we analysed the protein expression profile of the lung in the hypoxia + SPM and hypoxia groups after the comparative proteomics experiment. In this study, proteomic data were acquired by TMT-based LC-MS/MS analysis. As a result, a total of 44,919 peptides derived from 6658 proteins were identified through a regular search of the proteome database with Mascot 2.6 and Proteome Discoverer 2.1 software. Among the identified proteins, 28 proteins were differentially altered, with ratios >1.2 or <0.83, and

Table 2. Differentially expressed proteins with increased or decreased expression in lung from hypoxia + SPM group and hypoxia group.

Accession no.	Gene name	Protein description	Fold change	p Value
Q62715	Defa	Neutrophil antibiotic peptide NP-2	1.48	.048
D4AAP6	Mn1	Transcriptional regulator	1.40	.028
Q5RJS2	Rhoj	Ras homologue family member J	1.28	.005
G3V8A4	Mtr	Methyltransferase	1.27	.026
P35444	Comp	Cartilage oligomeric matrix protein	1.27	.038
G3V7D0	Mmp8	Matrix metalloproteinase	1.26	.027
P10959	Ces1c	Carboxylesterase 1C	1.23	.023
F1LVC4	Tigd2	Tigger transposable element-derived 2	1.20	.029
D3ZJA8	Cnep1r1	CTD nuclear envelope phosphatase 1	0.83	.025
Q8VH49	Higd1a	HIG1 domain family member 1A	0.83	.038
G3V7J9	Adh7	Alcohol dehydrogenase class 4	0.83	.015
D3ZY68	Gatc	Glutamyl-tRNA (Gln) amidotransferase	0.82	.029
Q4V8J1	Ppip5k2	Uncharacterized protein	0.82	.012
Q3B8N9	Bphl	Biphenyl hydrolase-like	0.82	.015
A0A0G2JSU8	Cyp2d1	Cytochrome P450 2D1	0.81	.014
B4F7B6	Bmi1	BMI1 proto-oncogene	0.81	.009
B2RZ23	Cenpa	Centromere protein A	0.80	.022
P84586	Rbmxrtl	RNA-binding motif protein	0.80	.038
Q02974	Khk	Ketohexokinase	0.80	.008
Q811A3	Plod2	Procollagen-lysine	0.80	.010
Q4G064	Coq5	Methylase	0.80	.016
F1LN38	Selenow	Selenoprotein W	0.79	.019
F1M7P4	Prph	Peripherin	0.79	.014
Q5U3Y7	Tmem97	Sigma intracellular receptor 2	0.79	.027
D4A6W9	Capsl	Calcyphosine-like	0.76	.028
A0A0A1FZ38	ND3	NADH-ubiquinone oxidoreductase chain 3	0.75	.018
P02692	Fabp1	Fatty acid-binding protein	0.52	.042
P00884	Aldob	Fructose-bisphosphate aldolase B	0.49	.021

they were used to create a protein list that was further filtered through statistical significance criteria (p-value < 0.05). A total of 8 upregulated and 20 downregulated proteins were identified in the hypoxia + SPM group compared with the hypoxia group (Table 2).

The separation of SDS-PAGE strip for each sample was clear (Figure 2(A)). The volcano plot in Figure 2(B) also presents the differential expression of proteins. For all 28 differentially expressed proteins, the frequency distribution of the log2-transformed A/B ratios in each group fit a normal distribution (Figure 2(C)). The hierarchical clustering heat map in Figure 2(D) shows the differentially expressed proteins in each group and the functional clustering analysis of different proteins. Hierarchical clustering indicated that there were two main branches, i.e., the hypoxia + SPM (A) and hypoxia (B) groups. From these data, it was clear that the samples from the hypoxia + SPM and hypoxia groups were clustered into their respective categories.

Annotation analysis of the differentially expressed proteins

We submitted all differentially expressed proteins to GO enrichment and KEGG pathway annotation. The annotated proteins were strongly enriched in the GO categories of fructose catabolic process, response to fructose, DNA methylation, inositol metabolic process, rough endoplasmic reticulum membrane, antioxidant activity, etc. (Figure 3(A)). To gain insights into the functional differences between the lung proteomes of the hypoxia + SPM group and those of the hypoxia group, the dysregulated proteins were mainly mapped to KEGG pathways. The enriched KEGG pathways were fructose and mannose metabolism, glycolysis/gluconeogenesis, biosynthesis of secondary metabolites, ubiquinone and other terpenoid-quinone biosynthesis and biosynthesis of amino acids (Figure 3(B)). Notably, the most dysregulated proteins were related to fructose catabolism or

metabolism, which implied that some significantly altered proteins/enzymes in the lung under high-altitude hypobaric hypoxia conditions were generally related to fructose catabolism or metabolism. The protein-protein interaction (PPI) network analysis with the IntAct database (http://www.ebi.ac.uk/intact/main.xhtml) and CytoScape software (version number: 3.2.1) obviously revealed that one crosstalk signalling cluster was related to fructose catabolism or metabolism (Figure 3(C)).

Validation of proteomics results

Six proteins, i.e., Mmp8, Fabp1, Bmi1, Aldob, Adh7, and Khk, were chosen to validate the TMT-based proteomics quantitative results using RT-qPCR according to the following selection criteria: upregulation or downregulation in all the replicated analyses, potential functional significance in high-altitude hypobaric hypoxia and different functional categories or pathways. Figure 4 displays the validation results. In line with the proteomic results, Mmp8 levels were increased in the hypoxia + SPM group compared to the hypoxia group ($p < 0.01$) (Figure 4(A)), whereas Fabp1, Bmi1, Aldob, Adh7 and Khk were notably downregulated ($p < 0.01$ or 0.001) (Figure 4(B–F)). Some differentially expressed proteins were strongly enriched in the GO categories of antioxidant activity, so the SOD and MDA related to antioxidant activity was also tested in the lung. The results indicated that the SOD content was significantly increased ($p < 0.01$) (Figure 4(G)) and that the MDA level was significantly decreased in the hypoxia + SPM group compared with the hypoxia group ($p < 0.05$) (Figure 4(H)).

Discussion

Medicinal plants commonly contain many bioactive constituents that have multiple biological activities. Rosmarinic acid is an abundant phenolic ester and has reported a range of biological
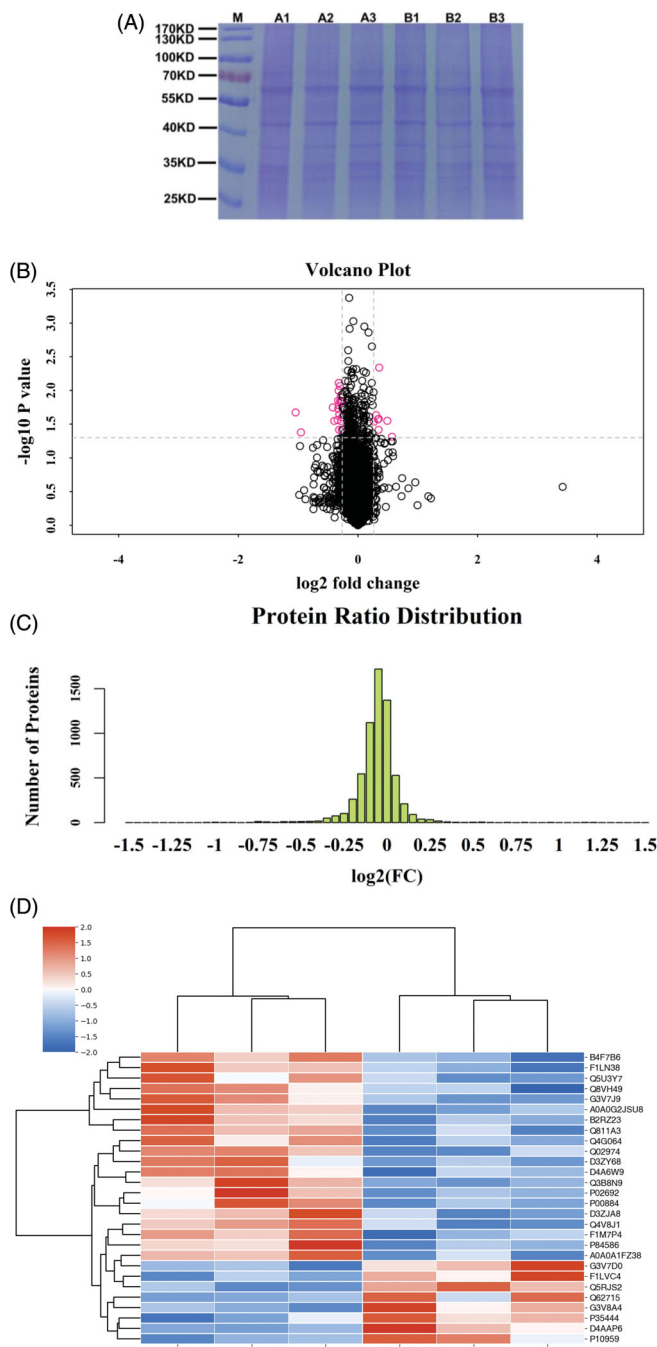
Figure 2. Characteristics of the identified proteins in hypoxia + SPM group and hypoxia group. (A) The result of SDS-PAGE. (B) The differentially expressed proteins are visualised by volcano plot. A protein with a fold change >1.2 or <0.83 and $p < .05$ is regarded as an up- or downregulated protein, which is coloured in red. The identified proteins with no significant changes are plotted in grey. Proteins with up- or downregulated abundance are shown on the right-hand side and left-hand side of the figure, respectively. (C) The quantitative ratio histogram of quantitative proteins. (D) Hierarchical clustering heat map of the 28 differentially expressed proteins. The colour of blue and red represent the up- and downregulated proteins, respectively. A1, A2, and A3, 3 replicates of hypoxia + SPM; B1, B2, and B3, 3 replicates of hypoxia. A/B represents hypoxia + SPM/hypoxia group.

effects of anti-diabetes (Ngo et al. 2018), anti-inflammatory, and anticancer activities (Amoah et al. 2016). Salvianolic acid B is one of abundant molecule isolated from the aqueous fraction of *S. miltiorrhiza* and has been shown to exert various antioxidative, anti-inflammatory (Chen et al. 2011), antitumour (Wang et al.

2013; Sha et al. 2018), and anti-emphysema (Dhapare and Sakagami 2018) effects. In the present study, we demonstrated that extracts from SPM contain two main components, rosmarinic acid and salvianolic acid B. The bioactivity of SPM extract may be associated with the components.

Compared with low altitude regions, high altitude regions have significantly decreased atmospheric pressure and partial oxygen pressure (Jacobsen 2008). HAPH is a severe health consequence of chronic exposure to hypoxia with a prevalence of up to 15% (Leon-Velarde et al. 2005). Herbal medicines play an important role in primary health care in many low- and middle-income countries. The main pharmacological activities of SPM are treating angina pectoris, stroke, atherosclerosis, myocardial infarction, liver fibrosis and hepatitis (Fei et al. 2017; Yu et al. 2018). In the present study, we demonstrated that SPM exhibits significant antihypoxia effects. To clarify the antihypoxia mechanism of SPM, we conducted TMT-based comparative proteomics analysis to analyse the differences in the lung proteomics profiles between the hypoxia + SPM groups and the hypoxia groups. In total, we identified 28 significantly altered (20 downregulated and 8 upregulated) proteins. Rhoj belongs to the super-family of small G proteins. Rhoj is abundantly expressed in vascular endothelial cells and has been shown to participate in a number of endothelial-cell related pathophysiological processes including angiogenesis and hypoxia (Kaur et al. 2011; Kim et al. 2014; Wilson et al. 2014; Liu et al. 2018). The blocking of endothelial Rhoj has been proposed as a novel anti-angiogenesis approach (Kim et al. 2014). MMP activity is crucial in the healthy lung for physiological processes (Dejonckheere et al. 2011). Lung disorders are associated with a high degree of oxidative stress, and MMP8 is highly sensitive to activation by reactive oxygen species (ROS) (Saari et al. 1992). MMP8 plays an anti-inflammatory role in both acute and chronic lung disorders through modulating numerous inflammatory mediators and clearing inflammatory cells from the site of infection (Dejonckheere et al. 2011). SPM can promote angiogenesis and exert an anti-inflammatory role through upregulating Rhoj and Mmp8 expression. And according to bioinformatics analysis, several annotated differentially expressed proteins were enriched in fructose catabolism or metabolism, antioxidative stress, and glycolysis/gluconeogenesis. These proteins are involved in the antihypoxia mechanism of SPM under the influence of hypobaric hypoxia.

Expression of antioxidant proteins

The high altitude exposure results under decreased partial pressure of oxygen and enhanced formation of ROS through mitochondrial electron transport chains, xanthine oxidase/reductase, NADPH oxidase, nitric oxide synthase enzymes, and inflammatory process (Dosek et al. 2007; Winterbourn 2008; Arya et al. 2013), which cause oxidative stress (Jayalakshmi et al. 2005; Maiti et al. 2006). This hypoxia-induced redox imbalance is a primary factor for lung pathological processes, such as increased pulmonary artery pressure, vascular proliferation, edoema, right heart failure and inflammation (Rosanna and Salvatore 2012; Sylvester et al. 2012; Tuder and Petrache 2012). Oxidative stress-related proteins are known to be controlled in redox regulation. Exposure to high altitude appears to decrease the activity and cellular defence systems of antioxidant enzymes (Ramanathan et al. 2005). A previous study reported that proteins involved in oxidoreductase activity were upregulated under hypoxia (Bousquet et al. 2015). In this study, SPM showed clear
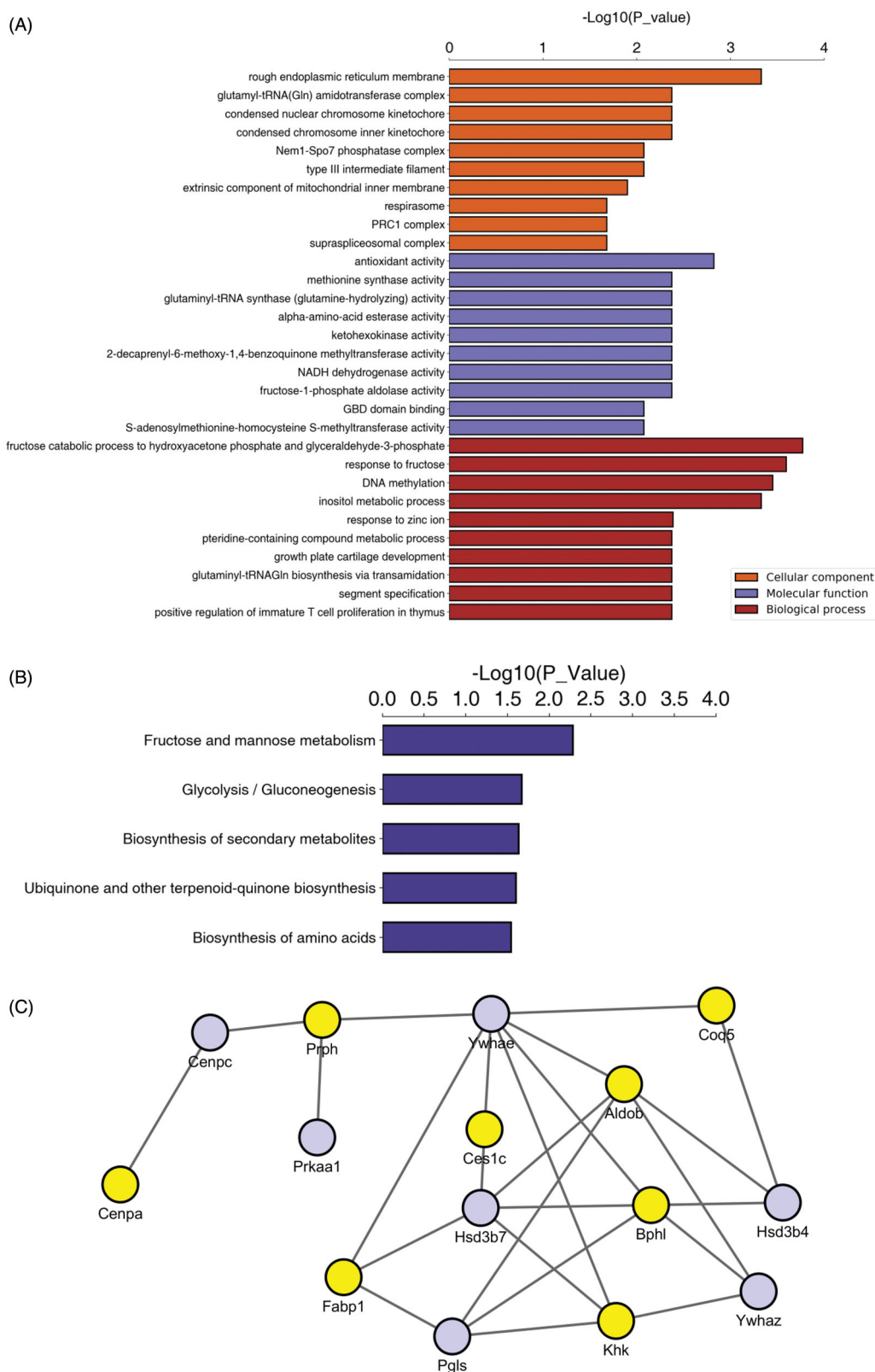
Figure 3. Enrichment analysis of the differentially expressed proteins. (A) GO term enrichment analysis of the differentially expressed proteins in cellular component, molecular function, and biological process. (B) Differentially expressed proteins corresponding to pathways analysed by KEGG pathway enrichment. (C) Analysis of protein – protein interaction network of the differentially expressed proteins. IntAct database and Cytoscape software were used to annotate and visualise functional interactions of all the 28 differentially expressed proteins.

antihypoxia effects with decreased mPAP and HIF-1α mRNA and improved HAPH pathology. SPM reduced oxidoreductase activity by downregulating the expression of Adh7, Cyp2d1, Plod2, Selenow, ND3 and Fabp1 according to GO annotation; meanwhile, SPM could effectively inhibit oxidative damage by enhancing antioxidant (SOD) levels and reducing oxidative stress
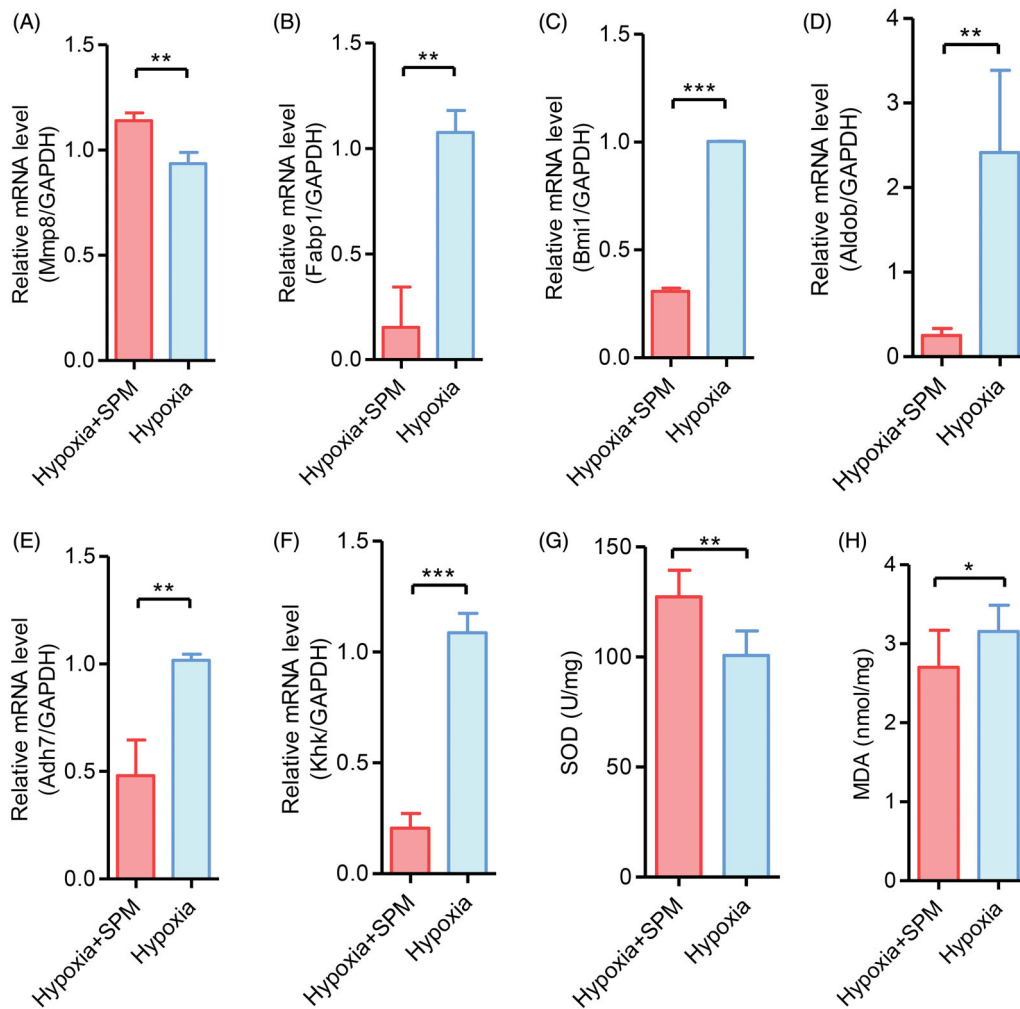
Figure 4. Validations of differentially changed proteins by RT-qPCR, and the levels of SOD and MDA were detected using colorimetric method. (A) Mmp8 ($n=6$), (B) Fabp1 ($n=6$), (C) Bmi1 ($n=6$), (D) Aldob ($n=6$), (E) Adh7 ($n=6$), (F) Khk ($n=6$), (G) SOD ($n=10$), and (H) MDA ($n=10$). Data represent the mean ± SD. $^*p<.05$, $^{**}p<.01$, $^{***}p<.001$.

(MDA) levels. Our results suggest that SPM can confer protection against hypoxia-induced oxidative stress by inhibiting oxidoreduction systems.

Expression of proteins associated with fructose metabolism

Differential proteomic results showed the downregulation of Khk and Aldob, proteins related to fructose metabolism. Fructose is a natural monosaccharide broadly used in modern society. Fructose is absorbed *via* two major facilitative glucose transporters: GLUT5 and GLUT2 (Pan and Kong 2018). Fructose metabolism requires the coordinated action of 2 enzymes, ketohexokinase (Khk), which phosphorylates fructose to form fructose 1-phosphate (Fru1-P), and aldolase B, which splits Fru1-P into dihydroxyacetone phosphate and glyceraldehydes (Lanaspa et al. 2018), thereby producing substrates for fatty acid synthesis. Fructose bypasses glycolysis, and fructose is utilised much faster than glucose in *de novo* lipogenesis (Samuel 2011); thus, the excessive intake of fructose is closely associated with metabolic diseases such as diabetes and obesity (Walker and Goran 2015). Therefore, the repression of fructose-induced fatty liver is a key strategy for the prevention of these metabolic diseases. In this report, through the use of comparative proteomics, we demonstrate that SPM inhibited fructose metabolism *via* the

downregulation of Khk and Aldob protein expression to prevent the lung injury associated with hypobaric hypoxia.

Conclusions

This study demonstrated that *Salvia przewalskii* has an antihypoxia effect on hypobaric hypoxia at high altitude by increasing antioxidant capacity through the inhibition of oxidoreduction systems and by inhibiting fructose metabolism through the downregulation of the Khk and Aldob proteins.

Disclosure statement

Supplementary materials

The proteomics data has been deposited at iProX database (IPX0001910000). The raw data of the 6658 protein (including the detailed gene name, molecular weight, score, coverage, peptides, unique peptides, GO annotation, KEGG pathway, enrichment analysis, fold changes, p value) is represented in Supplementary 1.

References

Amoah SK, Sandjo LP, Kratz JM, Biavatti MW. 2016. Rosmarinic acid–pharmaceutical and clinical aspects. Planta Med. 82(05):388–406.

Arya A, Sethy NK, Singh SK, Das M, Bhargava K. 2013. Cerium oxide nanoparticles protect rodent lungs from hypobaric hypoxia-induced oxidative stress and inflammation. Int J Nanomed. 8:4507–4520.

Barry PW, Pollard AJ. 2003. Altitude illness. BMJ. 326(7395):915–919.

Beall CM, Cavalleri GL, Deng L, Elston RC, Gao Y, Knight J, Li C, Li JC, Liang Y, McCormack M, et al. 2010. Natural selection on EPAS1 (HIF2) associated with low hemoglobin concentration in Tibetan highlanders. Proc Natl Acad Sci USA. 107(25):11459–11464.

Bousquet PA, Sandvik JA, Arntzen MØ, Jeppesen Edin NF, Christoffersen S, Krengel U, Pettersen EO, Thiede B. 2015. Hypoxia strongly affects mitochondrial ribosomal proteins and translocases, as shown by quantitative proteomics of HeLa Cells. Int J Proteomics. 2015:678527.

Chen T, Liu W, Chao X, Zhang L, Qu Y, Huo J, Fei Z. 2011. Salvianolic acid B attenuates brain damage and inflammation after traumatic brain injury in mice. Brain Res Bull. 84(2):163–168.

Dejonckheere E, Vandenbroucke RE, Libert C. 2011. Matrix metalloproteinase8 has a central role in inflammatory disorders and cancer progression. Cytokine Growth Factor Rev. 22(2):73–81.

Dhapare S, Sakagami M. 2018. Salvianolic acid B as an anti-emphysema agent I: *In vitro* stimulation of lung cell proliferation and migration, and protection against lung cell death, and *in vivo* lung STAT3 activation and VEGF elevation. Pulm Pharmacol Ther. 53:107–115.

Dosek A, Ohno H, Acs Z, Taylor AW, Radak Z. 2007. High altitude and oxidative stress. Respir Physiol Neurobiol. 158(2–3):128–131.

Fei YX, Wang SQ, Yang LJ, Qiu YY, Li YZ, Liu WY, Xi T, Fang WR, Li YM. 2017. *Salvia miltiorrhiza* Bunge (Danshen) extract attenuates permanent cerebral ischemia through inhibiting platelet activation in rats. J Ethnopharmacol. 207:57–66.

Hackett PH, Roach RC. 2001. High-altitude illness. N Engl J Med. 345(2):107–114.

Hao PP, Jiang F, Chen YG, Yang J, Zhang K, Zhang MX, Zhang C, Zhao YX, Zhang Y. 2015. Evidence for traditional Chinese medication to treat cardiovascular disease. Nat Rev Cardiol. 12(6):374–374.

Jacobsen D. 2008. Low oxygen pressure as a driving factor for the altitudinal decline in taxon richness of stream macroinvertebrates. Oecologia. 154(4):795–807.

Jayalakshmi K, Sairam M, Singh SB, Sharma SK, Ilavazhagan G, Banerjee PK. 2005. Neuroprotective effect of *N*-acetyl cysteine on hypoxia induced oxidative stress in primary hippocampal culture. Brain Res. 1046(1–2):97–104.

Kaur S, Leszczynska K, Abraham S, Scarcia M, Hiltbrunner S, Marshall CJ, Mavria G, Bicknell R, Heath VL. 2011. RhoJ/TCL regulates endothelial motility and tube formation and modulates actomyosin contractility and focal adhesion numbers. Arterioscler Thromb Vasc Biol. 31(3):657–664.

Kim C, Yang H, Fukushima Y, Saw PE, Lee J, Park JS, Park I, Jung J, Kataoka H, Lee D, et al. 2014. Vascular RhoJ is an effective and selective target for tumor angiogenesis and vascular disruption. Cancer Cell. 25(1):102–117.

Jia C, Han S, Wei L, Dang X, Niu Q, Chen M, Cao B, Liu Y, Jiao H. 2018. Protective effect of compound Danshen (*Salvia miltiorrhiza*) dripping pills alone and in combination with carbamazepine on kainic acid-induced temporal lobe epilepsy and cognitive impairment in rats. Pharm Biol. 56(1):217–224.

Lanaspa MA, Andres-Hernando A, Orlicky DJ, Cicerchi C, Jang C, Li N, Milagres T, Kuwabara M, Wempe MF, Rabinowitz JD, et al. 2018. Ketohexokinase C blockade ameliorates fructose-induced metabolic dysfunction in fructose-sensitive mice. J Clin Invest. 128(6):2226–2238.

Leon-Velarde F, Maggiorini M, Reeves JT, Aldashev A, Asmus I, Bernardi L, Ge RL, Hackett P, Kobayashi T, Moore LG, et al. 2005. Consensus statement on chronic and subacute high altitude diseases. High Alt Med Biol. 6(2):147–157.

Liu L, Chen J, Sun L, Xu Y. 2018. RhoJ promotes hypoxia induced endothelial-to-mesenchymal transition by activating WDR5 expression. J Cell Biochem. 119(4):3384–3393.

Maiti P, Singh SB, Sharma AK, Muthuraju S, Banerjee PK, Ilavazhagan G. 2006. Hypobaric hypoxia induces oxidative stress in rat brain. Neurochem Int. 49(8):709–716.

Ngo YL, Lau CH, Chua LS. 2018. Review on rosmarinic acid extraction, fractionation and its anti-diabetic potential. Food Chem Toxicol. 121:687–700.

Olson GE, Whitin JC, Hill KE, Winfrey VP, Motley AK, Austin LM, Deal J, Cohen HJ, Burk RF. 2010. Extracellular glutathione peroxidase (Gpx3) binds specifically to basement membranes of mouse renal cortex tubule cells. Am J Physiol Renal Physiol. 298(5):F1244–F1253.

Pan Y, Kong LD. 2018. High fructose diet-induced metabolic syndrome: Pathophysiological mechanism and treatment by traditional Chinese medicine. Pharmacol Res. 130:438–450.

Pratali L, Cavana M, Sicari R, Picano E. 2010. Frequent subclinical high-altitude pulmonary edema detected by chest sonography as ultrasound lung comets in recreational climbers. Crit Care Med. 38:1818–1823.

Ramanathan L, Gozal D, Siegel JM. 2005. Antioxidant response to chronic hypoxia in the rat cerebellum and pons. J Neurochem. 93(1):47–52.

Ribon A, Pialoux V, Saugy JJ, Rupp T, Faiss R, Debevec T, Millet GP. 2016. Exposure to hypobaric hypoxia results in higher oxidative stress compared to normobaric hypoxia. Respir Physiol Neurobiol. 223:23–27.

Rosanna DP, Salvatore C. 2012. Reactive oxygen species, inflammation, and lung diseases. CPD. 18(26):3889–3900.

Saari H, Sorsa T, Lindy O, Suomalainen K, Halinen S, Konttinen YT. 1992. Reactive oxygen species as regulators of human neutrophil and fibroblast interstitial collagenases. Int J Tissue React. 14(3):113–120.

Samuel VT. 2011. Fructose induced lipogenesis: from sugar to fat to insulin resistance. Trends Endocrinol Metab. 22(2):60–65.

Sha W, Zhou Y, Ling ZQ, Xie G, Pang X, Wang P, Gu X. 2018. Antitumor properties of salvianolic acid B against triple-negative and hormone receptor-positive breast cancer cells via ceramide-mediated apoptosis. Oncotarget. 9(91):36331–36343.

Soeda A, Park M, Lee D, Mintz A, Androutsellis-Theotokis A, McKay RD, Engh J, Iwama T, Kunisada T, Kassam AB, et al. 2009. Hypoxia promotes expansion of the CD133-positive glioma stem cells through activation of HIF-1alpha. Oncogene. 28(45):3949–3959.

Sylvester JT, Shimoda LA, Aaronson PI, Ward JP. 2012. Hypoxic pulmonary vasoconstriction. Physiol Rev. 92(1):367–520.

Tuder RM, Petrache I. 2012. Pathogenesis of chronic obstructive pulmonary disease. J Clin Invest. 122(8):2749–2755.

Walker RW, Goran MI. 2015. Laboratory determined sugar content and composition of commercial infant formulas, baby foods and common grocery items targeted to children. Nutrients. 7(7):5850–5867.

Wang H, Wang S, Cui D, Dong S, Tuo X, Liu Z, Liu Y. 2017. iTRAQ-based proteomic technology revealed protein perturbations in intestinal mucosa from manganese exposure in rat models. RSC Adv. 7(50):31745–31758.

Wang Z, Liu F, Ye S, Jiang P, Yu X, Xu J, Du X, Ma L, Cao H, Yuan C, et al. 2019. Plasma proteome profiling of high-altitude polycythemia using TMT-based quantitative proteomics approach. J Proteomics. 194:60–69.

Wang ZS, Luo P, Dai SH, Liu ZB, Zheng XR, Chen T. 2013. Salvianolic acid B induces apoptosis in human glioma U87 cells through p38-mediated ROS generation. Cell Mol Neurobiol. 33(7):921–928.

Wilson E, Leszczynska K, Poulter NS, Edelmann F, Salisbury VA, Noy PJ, Bacon A, Rappoport JZ, Heath JK, Bicknell R, et al. 2014. RhoJ interacts with the GIT-PIX complex and regulates focal adhesion disassembly. J Cell Sci. 127(14):3039–3051.

Winterbourn CC. 2008. Reconciling the chemistry and biology of reactive oxygen species. Nat Chem Biol. 4(5):278–286.

Wiśniewski JR, Zougman A, Nagaraj N, Mann M. 2009. Universal sample preparation method for proteome analysis. Nat Methods. 6(5):359–362.

Yang R, Xie T, Yang H, Turner S, Wu G. 2018. Historical trends of organochlorine pesticides (OCPs) recorded in sediments across the Tibetan Plateau. Environ Geochem Health. 40(1):303–312.

Yu J, Gao H, Wu C, Xu QM, Lu JJ, Chen X. 2018. Diethyl blechnic, a novel natural product isolated from *Salvia miltiorrhiza* Bunge, inhibits doxorubicin-induced apoptosis by inhibiting ROS and activating JNK1/2. IJMS. 19(6):1809.

Zhu Y, Xu H, Chen H, Xie J, Shi M, Shen B, Deng X, Liu C, Zhan X, Peng C. 2014. Proteomic analysis of solid pseudopapillary tumor of the pancreas reveals dysfunction of the endoplasmic reticulum protein processing pathway. Mol Cell Proteomics. 13(10):2593–2603.